Coordination and Scission of Alkynes on a Tungsten–Triosmium Framework. Crystal Structures of $(\eta^5\text{-}C_5H_5)WOs_3(CO)_{10}[\mu_3\text{-}\eta^2\text{-}C_2(C_6H_4CH_3)_2]H$ and $(\eta^5\text{-}C_5H_5)WOs_3(CO)_{10}[\mu_3\text{-}\eta^2\text{-}C_2(CO_2C_2H_5)_2]H$—Species with an Alkyne Ligand Bound to Os_3 and WOs_2 Faces of Tetrahedral WOs_3 Clusters[1]

Joon T. Park and John R. Shapley*

Department of Chemistry, University of Illinois, Urbana, Illinois 61801

Clifford Bueno, Joseph W. Ziller, and Melvyn Rowen Churchill*

Department of Chemistry, University at Buffalo, State University of New York, Buffalo, New York 14214

Received February 8, 1988

Reactions of $CpWOs_3(CO)_{12}H$ ($Cp = \eta^5\text{-}C_5H_5$) with various alkynes ($RC{\equiv}CR'$) produce two isomeric (symmetrical and/or unsymmetrical) alkyne complexes $CpWOs_3(CO)_{10}(\mu_3\text{-}\eta^2\text{-}C_2RR')H$ [R = R′ = H, Ph, Tol, CF_3, CO_2Et; R = Ph, R′ = Tol; R = Ph, R′ = CO_2Et] (Ph = C_6H_5, Tol = $p\text{-}C_6H_4CH_3$) depending on the substituents R and R′ of alkynes. Some of the symmetrical isomers (R = CF_3, CO_2Et) undergo irreversible thermal isomerization to the unsymmetrical isomers. The diarylalkyne complexes (R = R′ = Ph, Tol; R = Ph, R′ = Tol) undergo facile intramolecular $C{\equiv}C$ bond scission reactions after CO loss by Me_3NO to yield the corresponding dialkylidyne clusters $CpWOs_3(CO)_9(\mu_3\text{-}CR)(\mu_3\text{-}CR')H$ in ca. 60% yield along with alkyne–oxo clusters $CpWOs_3(CO)_8(\mu\text{-}O)(\mu_3\text{-}\eta^2\text{-}C_2RR')H$ in ca. 10% yield. The isomeric alkyne complexes, alkyne–oxo clusters, and dialkylidyne clusters have been isolated as crystalline solids and have been characterized by spectroscopic (infrared, mass, ^1H and ^{13}C NMR) data. $CpWOs_3(CO)_{10}(\mu_3\text{-}\eta^2\text{-}C_2Tol_2)H$ crystallizes in the centrosymmetric monoclinic space group $P2_1/n$ (No. 14) with $a = 23.600$ (5) Å, $b = 9.343$ (2) Å, $c = 28.774$ (4) Å, $\beta = 97.39$ (2)°, $V = 6292$ (2) Å^3, and $Z = 8$. The structure solution converged with $R_F = 5.0\%$ for those 4223 reflections with $|F_o| > 3.0\sigma(|F_o|)$ and $R_F = 8.6\%$ for all 5816 independent data (Mo K$\bar{\alpha}$, $2\theta = 4.5\text{–}40.0°$). There are two essentially equivalent molecules in the crystallographic asymmetric unit. Each consists of a tetrahedral WOs_3 cluster in which the C_2Tol_2 ligand is bound to an Os_3 face (π-bonded to Os(3) and σ-bonded to Os(1) and Os(2)). Os(3) bears two terminal carbonyl ligands, while Os(1) and Os(2) each have three. The W atom has two CO ligands, one of which is involved in a semibridging manner with the otherwise "electron-poor" Os(3); the hydride ligand (not located directly) is believed to span the Os(1)–Os(2) linkage. $CpWOs_3(CO)_{10}(\mu_3\text{-}\eta^2\text{-}C_2(CO_2Et)_2)H$ crystallizes in the centrosymmetric triclinic space group $P\bar{1}$ (No. 2) with $a = 9.121$ (4) Å, $b = 9.964$ (3) Å, $c = 15.729$ (4) Å, $\alpha = 85.63$ (2)°, $\beta = 83.30$ (3)°, $\gamma = 85.74$ (3)°, $V = 1412.5$ (8) Å^3, and $Z = 2$. Refinement converged with $R_F = 4.87\%$ for those 4240 data with $|F_o| > 3.0\sigma(|F_o|)$ and $R_F = 5.55\%$ for all 4868 independent data (Mo K$\bar{\alpha}$, $2\theta = 4.5\text{–}50.0°$). The molecule contains a tetrahedral WOs_3 cluster, with the $C_2(CO_2Et)_2$ ligand now bound to a WOs_2 face (π-bonded to W and σ-bonded to Os(1) and Os(3)). The Os atoms each bear three terminal CO ligands, while the W atom has only one.

Introduction

Synthesis of alkyne ($RC{\equiv}CR'$) substituted clusters and the scission of alkyne $C{\equiv}C$ bonds on a cluster have been of current interest due to their potential as models for the $C{\equiv}C$ bond activation on metal surfaces.[2,3] Relatively few reactions of mixed-metal clusters with alkynes have been reported; however, previous results have shown that alkyne coordination to tetrametallic mixed-metal clusters typically results in metal–metal bond cleavage to give pseudooctahedral (closo) structures with a $\mu_4\text{-}\eta^2$-bonding mode I.[2,3e,f]

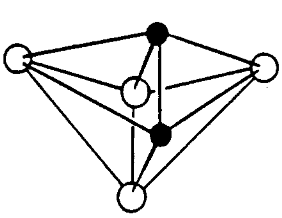

I

$\mu_4\text{-}\eta^2$-bonding mode

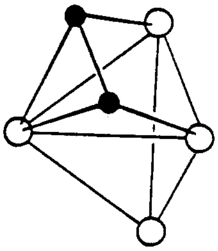

II

$\mu_3\text{-}\eta^2$-bonding mode

We now report full details of the preparation and characterization of tetrametallic alkyne complexes that display the $\mu_3\text{-}\eta^2$-bonding mode II, which is commonly observed only in trimetallic alkyne complexes.[2] The cluster compound $CpWOs_3(CO)_{12}H$[5] reacts with various alkynes

---

[1] Structural Studies on Polynuclear Osmium Carbonyl Hydrides. 35. Recent previous parts are the following: (a) Part 34. Churchill, M. R.; Fettinger, J. C.; Hollander, F. J.; Lashewycz-Rubycz, R. A. *J. Organomet. Chem.* **1988**, *340*, 367. (b) Part 33. Chi, Y.; Shapley, J. R.; Churchill, M. R.; Li, Y.-J. *Inorg. Chem.* **1986**, *25*, 4165. (c) Part 32. Churchill, M. R.; Li, Y.-J. *J. Organomet. Chem.* **1985**, *294* 367. (d) Part 31. Churchill, M. R.; Li, Y.-J. *J. Organomet. Chem.* **1985**, *291*, 61. (e) Part 30. Yeh, W.-Y., Shapley, J. R.; Li, Y.-J.; Churchill, M. R. *Organometallics* **1985**, *4*, 767.

[2] Sappa, E.; Tiripicchio, A.; Braunstein, P. *Chem. Rev.* **1983**, *83*, 203.

[3] (a) Allison, N. T.; Fritch, J. R.; Vollhardt, K. P. C.; Walborsky, E. C. *J. Am. Chem. Soc.* **1983**, *105*, 1384. (b) Clauss, A. D.; Shapley, J. R.; Wilker, C. N.; Hoffmann, R. *Organometallics* **1984**, *3*, 619. (c) Shapley, J. R.; McAteer, C. H.; Churchill, M. R.; Biondi, L. V. *Ibid.* **1984**, *3*, 1595. (d) Chi, Y.; Shapley, J. R. *Ibid.* **1985**, *4*, 1900. (e) Fox, J. R.; Gladfelter, W. L.; Geoffroy, G. L.; Tavanairpour, I.; Abdel-Mequid, S.; Day, V. W. *Inorg. Chem.* **1981**, *20*, 3230. (f) Roland, E.; Vahrenkamp, H. *Organometallics* **1983**, *2*, 184.

[4] (a) Park, J. T.; Shapley, J. R.; Churchill, M. R.; Bueno, C. *J. Am. Chem. Soc.* **1983**, *105*, 6182. (b) Churchill, M. R.; Bueno, C.; Park, J. T.; Shapley, J. R. *Inorg. Chem.* **1984**, *23*, 1017.

[5] Churchill, M. R.; Hollander, F. J.; Shapley, J. R.; Foose, D. S. *J. Am. Chem. Soc.* **1978**, *100*, 534.

0276-7333/88/2307-2307$01.50/0

to form two isomeric alkyne derivatives (symmetrical and/or unsymmetrical), $CpWOs_3(CO)_{10}(\mu_3\text{-}\eta^2\text{-}C_2RR')H$, of configuration II. Both isomers therefore show a capped square pyramidal (nido) structure, where one metal caps a triangular face of the square pyramid defined by the remaining M_3C_2 skeletal atoms. The symmetrical isomers with electron-withdrawing alkynes (R = R′ = CF_3, CO_2Et) undergo irreversible isomerization to the unsymmetrical isomers upon heating. The diaryl-substituted alkyne complexes undergo intramolecular alkyne scission reactions upon pyrolysis to produce the corresponding dialkylidyne clusters $CpWOs_3(CO)_9(\mu_3\text{-}CR)(\mu_3\text{-}CR')H$[4a] along with the alkyne–oxo clusters $CpWOs_3(CO)_8(\mu\text{-}O)(\mu_3\text{-}\eta^2\text{-}C_2RR')H$ as minor products (ca. 10% yield). A preliminary account of some of this work has been published.[4a]

Experimental Section

Materials. Solvents were reagent grade and were used as purchased, except that acetonitrile and dichloromethane were distilled from phosphorus pentoxide and toluene was dried by distillation from sodium metal and benzophenone.

Diphenylacetylene (99%), diethyl acetylenedicarboxylate (99%), 4-methylbenzophenone (97%), phenylpropiolic acid (97%), and trimethylamine oxide dihydrate (98%) were purchased from Aldrich; *tert*-butyl hypochlorite was purchased from Frinton Labs, ethyne (99.6% min.) from Matheson, hexafluoro-2-butyne from PCR Research Chemicals, and ^{13}C-enriched carbon monoxide (90%) from Monsanto Research Corp. Anhydrous trimethylamine oxide (mp 225–230 °C) was obtained from trimethylamine oxide dihydrate by sublimation (three times) at 90–100 °C in vacuo. Phenyl-*p*-tolylacetylene was synthesized by the reaction of 4-methylbenzophenone with (trimethylsilyl)diazomethane promoted by *n*-butyllithium as described by Colvin.[6] Ethyl phenylpropiolate was prepared by acid-catalyzed esterification of phenylpropiolic acid with ethanol.[7] Di-*p*-tolylacetylene[8] and $CpWOs_3(CO)_{12}H$[5] were prepared by literature methods. Carbon-13 enriched $PhC{\equiv}CPh$ (ca. 50%) was prepared from ^{13}CO-enriched benzophenone obtained from the reaction between phenyllithium and ^{13}C-enriched carbon monoxide.[9]

General Procedures. All reactions were carried out under an atmosphere of nitrogen in oven-dried glassware. The progress of the reactions was monitored by analytical thin-layer chromotography (precoated TLC plates, Silica Gel 60 F-254, E. Merck). Preparative TLC was carried out by using ca. 2-mm glass-backed silica gel plates (10 × 20 cm) prepared from silica Gel G (Type 60, E. Merck). A mixture of pentane and dichloromethane (3:2) was used as an eluting solvent for the preparative TLC unless specified otherwise.

Infrared spectra were obtained on a Perkin-Elmer 281B spectrophotometer. ^1H NMR (360 MHz), ^{13}C NMR (90 MHz), and ^{19}F NMR (340 MHz) were recorded on a Nicolet NT-360 spectrometer. $Cr(acac)_3$ (ca. 0.02 M) was added to each ^{13}C sample as a shiftless relaxation reagent. Chemical shifts of ^{19}F NMR are given in parts per million relative to CCl_3F as an internal standard. Mass spectra were recorded by the staff of the Mass Spectroscopy Laboratory of the School of Chemical Sciences at the University of Illinois using either Varian MAT CH-5 or Varian MAT-731 mass spectrometers. All m/z values are referenced to ^{184}W and ^{192}Os. Microanalytical data were provided by the Microanalytical Laboratory of the School of Chemical Sciences at the University of Illinois.

Reaction of $CpWOs_3(CO)_{12}H$ with Di-*p*-tolylacetylene. A red dichloromethane (30 mL)–acetonitrile (10 mL) solution of $CpWOs_3(CO)_{12}H$ (43.7 mg, 0.0409 mmol) was treated with an acetonitrile solution (5 mL) of sublimed Me_3NO (3.3 mg, 0.044 mmol). After evaporation of the solvent in vacuo, to the greenish blue toluene solution (70 ml) of the residue was added an excess of di-*p*-tolylacetylene (25.1 mg, 0.122 mmol) at room temperature. The resulting orange solution was heated to reflux for 1 h. After evaporation of the solvent, purification by preparative TLC afforded $CpWOs_3(CO)_{10}(\mu_3\text{-}\eta^2\text{-}C_2Tol_2)H$ (**1a**, 25.6 mg, 0.0196 mmol, 48%, R_f 0.20) as an orange crystalline solid. Minor bands (<5% yields) were observed on the TLC plate but were not characterized. Recrystallization from dichloromethane–pentane gave an analytically pure sample of compound **1a**. A single crystal suitable for an X-ray analysis was grown by slow evaporation from hexane–dichloromethane at room temperature: IR (CCl_4) ν(CO) 2080 (vw), 2064 (s), 2019 (vs), 2005 (w), 1988 (m), 1960 (w) cm^{-1}; ^1H NMR ($CDCl_3$, 25 °C) δ 6.78–6.89 (m, 8 H), 5.50 (s, 5 H), 2.25 (s, 6 H), −21.23 (s, 1 H); MS (field desorption), m/z 1312 (M^+). Anal. Calcd for $C_{31}H_{20}O_{10}WOs_3$: C, 28.49; H, 1.54. Found: C, 28.46; H, 1.37.

Reaction of $CpWOs_3(CO)_{12}H$ with Diphenylacetylene. The reaction of $CpWOs_3(CO)_{12}H$ (49.2 mg, 0.0425 mmol) with diphenylacetylene (19.0 mg, 0.107 mmol) was carried out in a similar manner to that described above. After purification by preparative TLC, $CpWOs_3(CO)_{10}(\mu_3\text{-}\eta^2\text{-}C_2Ph_2)H$ (**2a**, 24.4 mg, 0.0191 mmol, 45%, R_f 0.2) was isolated as an orange-red solid: IR (CCl_4) ν(CO) 2082 (vw), 2065 (s), 2020 (vs), 2005 (w), 1988 (m), 1960 (w) cm^{-1}; ^1H NMR (CD_2Cl_2, 25 °C) δ 6.94–7.12 (m, 10 H), 5.57 (s, 5 H), −21.15 (s, 1 H); MS (70 eV), m/z 1284 (M^+). Anal. Calcd for $C_{29}H_{16}O_{10}WOs_3$: C, 27.24; H, 1.26. Found: C, 27.18; H, 1.07.

Reaction of $CpWOs_3(CO)_{12}H$ with Phenyl-*p*-tolylacetylene. The same procedure was followed as for the preparation of **1a**. Orange $CpWOs_3(CO)_{10}(\mu_3\text{-}\eta^2\text{-}C_2PhTol)H$ (**3a**, 21.8 mg, 0.0169 mmol, 42%, R_f 0.2) was obtained from $CpWOs_3(CO)_{12}H$ (46.6 mg, 0.0403 mmol) after isolation by preparative TLC: IR (C_6H_{12}) ν(CO) 2082 (vw), 2065 (s), 2020 (vs), 2013 (w), 2007 (w), 1987 (s), 1962 (w) cm^{-1}; ^1H NMR (CD_2Cl_2, 25 °C) δ 6.80–7.14 (m, 9 H), 5.56 (s, 5 H), 2.26 (s, 3 H), −21.15 (s, 1 H); MS (field desorption), m/z 1298 (M^+).

Reaction of $CpWOs_3(CO)_{12}H$ with Ethyl Phenylpropiolate. The reaction of $CpWOs_3(CO)_{12}H$ (20.9 mg, 0.0181 mmol) and ethyl phenylpropiolate (10.7 mg, 0.0614 mmol) was carried out following a procedure similar to that for **1a**. Evaporation of the solvent and separation by preparative TLC (eluted two times with pentane–dichloromethane, 1:1) gave orange $CpWOs_3(CO)_{10}[\mu_3\text{-}\eta^2\text{-}C_2Ph(CO_2Et)]H$ (**5a**, 3.9 mg, 0.031 mmol, 17%, R_f 0.1) and a mixture of two dark red isomers $CpWOs_3(CO)_{10}[\mu_3\text{-}\eta^2\text{-}C_2Ph(CO_2Et)]H$ (**5b** and **5c** (5:2 ratio), 7.5 mg, 0.0059 mmol, 33%, R_f 0.2).

Compound **5a**: IR (C_6H_{12}) ν(CO) 2090 (vw), 2069 (s), 2031 (vs), 2018 (m), 2010 (w), 1991 (s), 1967 (w), 1696 (vw) cm^{-1}; ^1H NMR (CD_2Cl_2, 25 °C) δ 7.11–7.32 (m, 5 H), 5.56 (s, 5 H), 4.00 (q, 2 H, J = 7.1 Hz), 1.01 (t, 3 H, J = 7.1 Hz), −21.37 (s, 1 H).

Mixture of **5b** and **5c** (5:2): IR (C_6H_{12}) ν(CO) 2087 (m), 2062 (s), 2036 (vs), 2013 (m), 2011 (sh), 2005 (m), 1991 (vw), 1986 (w), 1968 (w), 1957 (vw), 1727 (vw), 1697 (vw) cm^{-1}; ^1H NMR (CD_2Cl_2, 25 °C) δ 6.97–7.33 (m, 10 H, **5b** and **5c**), 5.34 (s, 5 H, **5b**), 5.33 (s, 5 H, **5c**), 3.98 (q, 2 H, **5c**), 3.94 (q, 2 H, **5b**), 1.05 (t, 3 H, J = 7.1 Hz, **5c**), 1.00 (t, 3 H, J = 7.1 Hz, **5b**), −21.69 (s, 1 H, **5c**), −22.26 (s, 1 H, **5b**).

Reaction of $CpWOs_3(CO)_{12}H$ with Diethyl Acetylenedicarboxylate. The same procedure was used as for the preparation of **1a**, except that a toluene solution of the reaction mixture was refluxed for 0.5 h using $CpWOs_3(CO)_{12}H$ (63.7 mg, 0.0551 mmol) with diethyl acetylenedicarboxylate (30 μL, 0.19 mmol). The solvent was evaporated, and the crude product was purified by preparative TLC (dichloromethane) to provide a mixture of two isomers $CpWOs_3(CO)_{10}[\mu_3\text{-}\eta^2\text{-}C_2(CO_2Et)_2]H$ (**6a** and **6b**, 34.3 mg, 49%, R_f 0.1) as a red solid. Recrystallization from pentane–dichloromethane at room temperature gave orange crystals of isomer **6a** (18.5 mg, 14.6 mmol, 26%). The red supernatant was evaporated, and dark red crystals of isomer **6b** (15.8 mg, 0.0124 mmol, 23%) were isolated after recrystallization from methanol–dichloromethane at −10 °C. Crystals of **6b** suitable for X-ray analysis were grown from methanol–dichloromethane at −10 °C.

Compound **6a**: IR (CCl_4) ν(CO) 2094 (vw), 2076 (s), 2037 (vs), 2019 (w), 1995 (w), 1975 (w), 1710 (vw) cm^{-1}; ^1H NMR ($CDCl_3$, 25 °C) δ 5.52 (s, 5 H), 4.21 (q, 4 H, J = 7.2 Hz), 1.27 (t, 6 H, J

---

(6) Colvin, E. W.; Idamill, B. J. *J. Chem. Soc., Perkin Trans. 1* **1977**, 869.

(7) Roberts, R. M., Rodewald, L. B., Wingrove, A. S., Eds. *An Introduction to Modern Experimental Organic Chemistry*, 2nd ed.; Holt, Rinehart and Winston: New York, 1900; p 298.

(8) Cope, A. C.; Smith, D. S.; Cotter, R. J. *Organic Synthes*; Wiley: New York, 1963; Coll. Vol. 4, p 337.

(9) Trzupek, L. S.; Newirth, T. L.; Kelly, E. G.; Sbarbati, N. E.; Whitesides, G. M. *J. Am. Chem. Soc.* **1973**, *95*, 8118.

= 7.2 Hz), −21.62 (s, 1 H); MS (field desorption), *m/z* 1276 (M$^+$). Anal. Calcd for $C_{23}H_{16}O_{14}WOs_3$: C, 21.74; H, 1.27. Found: C, 21.75; H, 1.17.

Compound **6b**: IR (C_6H_{12}) ν(CO) 2090 (m), 2065 (s), 2037 (vs), 2018 (m), 2011 (m), 2007 (m), 1995 (w), 1979 (vw), 1962 (vw), 1949 (m), 1708 (vw), 1698 (vw) cm^{-1}; ^{1}H NMR ($CDCl_3$, 25 °C) δ 5.48 (s, 5 H), 4.14–4.21 (m, 4 H), 1.29 (t, 3 H, J = 7.2 Hz), 1.26 (t, 3 H, J = 7.2 Hz), −22.29 (s, 1 H); MS (field desorption), *m/z* 1276 (M$^+$). Anal. Calcd for $C_{23}H_{16}O_{14}WOs_3$: C, 21.74; H, 1.27. Found: C, 21.67; H, 1.12.

Reaction of CpWOs$_3$(CO)$_{12}$H with Hexafluoro-2-butyne. The reaction was carried out by a procedure similar to that for the preparation of **4a**,[4b] except that CpWOs$_3$(CO)$_{12}$H (30.6 mg, 0.0265 mmol) and hexafluoro-2-butyne (ca. 10 psig) were used. Purification by preparative TLC provided orange CpWOs$_3$(CO)$_{10}$[μ_3-η^2-$C_2(CF_3)_2$]H (**7a**, 2.4 mg, 0.0019 mmol, 7%, R_f 0.2) and red CpWOs$_3$(CO)$_{10}$[μ_3-η^2-$C_2(CF_3)_2$]H (**7b**, 12.6 mg, 0.00998 mmol, 38%, R_f 0.45).

Compound **7a**: IR (CCl_4) ν(CO) 2099 (vw), 2082 (s), 2043 (vs), 2028 (w), 2001 (m), 1985 (w) cm^{-1}; ^{1}H NMR ($CDCl_3$, 25 °C) δ 5.57 (s, 5 H), −21.65 (s, 1 H); ^{19}F NMR ($CFCl_3$, 25 °C) δ −54.6 (s, 6 F).

Compound **7b**: IR (CCl_4) ν(CO) 2097 (m), 2073 (s), 2044 (vs), 2028 (m), 2019 (m), 2015 (m), 2000 (w), 1994 (vw), 1969 (vw), 1956 (w) cm^{-1}; ^{1}H NMR ($CDCl_3$, 25 °C) δ 5.57 (s, 5 H), −22.43 (s, 1 H); ^{19}F NMR ($CFCl_3$, 25 °C) δ −47.5 (m, 3 F), −51.5 (m, 3 F).

Attempted Alkyne Exchange Reaction. A toluene solution of CpWOs$_3$(CO)$_{10}$[μ_3-η^2-$C_2(CO_2Et)_2$]H (isomer **5a**, 1.3 mg, 0.001 mmol) and di-*p*-tolylacetylene (1.9 mg, 0.009 mmol) was heated to reflux for 0.5 h. No indication of alkyne exchange was observed in monitoring the reaction by analytical TLC.

Alkyne Scission Reaction of 1a. An orange dichloromethane (30 mL)–acetonitrile (10 mL) solution of **1a** (37.1 mg, 0.0284 mmol) was treated with an acetonitrile solution (1 mL) of sublimed Me_3NO (2.3 mg, 0.0306 mmol). After evaporation of the solvent in vacuo, a toluene solution of the residue was heated to reflux for 1 h. Purification by preparative TLC afforded dark red CpWOs$_3$(CO)$_9$(μ_3-CTol)$_2$H (**1d**, 22.8 mg, 0.0178 mmol, 63%, R_f 0.6) and dark red CpWOs$_3$(CO)$_8$(μ-O)(μ_3-η^2-C_2Tol_2)H (**1e**, 3.0 mg, 0.0024 mmol, 8%, R_f 0.25).

Compound **1d**: IR (C_6H_{12}) ν(CO) 2072 (s), 2036 (vs), 2031 (vs), 1999 (w), 1991 (m), 1980 (m) cm^{-1}; ^{1}H NMR (CD_2Cl_2, 25 °C) δ 7.03–7.11 (m, 8 H), 5.40 (s, 5 H), 3.75 (s, 1 H, $^1J_{WH}$ = 89 Hz), 2.36 (s, 6 H); MS (70 eV), *m/z* 1284 (M$^+$), 1284–28*X*, *X* = 1–9 (M$^+$ − *X*CO). Anal. Calcd for $C_{30}H_{20}O_9WOs_3$: C, 28.18; H, 1.58. Found: C, 28.10; H, 1.56.

Compound **1e**: IR (C_6H_{12}) ν(CO) 2084 (s), 2049 (vs), 2022 (w), 2005 (vs), 1994 (m), 1982 (m), 1968 (m), 1938 (m) cm^{-1}; ^{1}H NMR ($CDCl_3$, 25 °C) δ 6.91–7.06 (m, 8 H), 5.78 (s, 5 H), 2.37 (s, 3 H), 2.26 (s, 3 H), −10.46 (s, 1 H); MS (field desorption), *m/z* 1272 (M$^+$).

Alkyne Scission Reaction of 2a. The reaction was carried out similar to that described for **1a** using CpWOs$_3$(CO)$_{10}$(μ_3-η^2-C_2Ph_2)H (38.4 mg, 0.030 mmol). Purification by preparative TLC provided dark red CpWOs$_3$(CO)$_9$(μ_3-CPh)$_2$H (**2d**, 22.5 mg, 0.0180 mmol, 60%, R_f 0.6) and dark red CpWOs$_3$(CO)$_8$(μ-O)(μ_3-η^2-C_2Ph_2)H (**2e**, 3.5 mg, 0.028 mmol, 9%, R_f = 0.25) after recrystallization from methanol–dichloromethane.

Compound **2d**: IR (C_6H_{12}) ν(CO) 2077 (s), 2041 (vs), 2037 (vs), 2003 (w), 1992 (m), 1881 (m) cm^{-1}; ^{1}H NMR (CD_2Cl_2, 25 °C) δ 7.14–7.32 (m, 10 H), 5.42 (s, 5 H), 4.00 (s, 1 H, $^1J_{WH}$ = 89 Hz); MS (field desorption), *m/z* 1256 (M$^+$). Anal. Calcd for $C_{28}H_{16}O_9WOs_3$: C, 26.89; M, 1.29. Found: C, 26.80; H, 1.16.

Compound **2e**: IR (C_6H_{12}) ν(CO) 2085 (s), 2050 (vs), 2022 (w), 2007 (vs), 1995 (m), 1983 (m), 1969 (m), 1940 (m) cm^{-1}; ^{1}H NMR (CD_2Cl_2, 25 °C) δ 6.89–7.12 (m, 10 H), 5.76 (s, 5 H), −10.47 (s, 1 H); MS (field desorption), *m/z* 1244 (M$^+$).

Alkyne Scission Reaction of 3a. The reaction was carried out by the procedure described for **1a** using CpWOs$_3$(CO)$_{10}$(μ_3-η^2-C_2PhTol)H (8.6 mg, 0.0067 mmol). Purification by preparative TLC gave CpWOs$_3$(CO)$_9$(μ_3-CPh)(μ_3-CTol)H (**3d**, 5.2 mg, 0.0041 mmol, 61%, R_f 0.6) as a dark red crystalline solid. The corresponding oxo compound was observed on the TLC plate but was not characterized: IR (C_6H_{12}) ν(CO) 2078 (s), 2041 (vs), 2036 (vs), 2011 (vw), 2003 (w), 1993 (m), 1981 (m) cm^{-1}; ^{1}H NMR (CD_2Cl_2, 25 °C) δ 7.04–7.31 (m, 9 H), 5.41 (s, 5 H), 3.89 (s, 1 H, $^1J_{WH}$ = 89 Hz), 2.36 (s, 3 H); MS (FAB), *m/z* 1270 (M$^+$), 1270–28*X*, *X* = 1–3 (M$^+$ − *X*CO).

Table I. Experimental Data for the X-ray Diffraction Studies on CpWOs$_3$(CO)$_{10}$(μ_3-η^2-C_2Tol_2)H (1a) and CpWOs$_3$(CO)$_{10}$(μ_3-η^2-$C_2(CO_2Et)_2$)H (6b)

(A) Crystal Parameters

	1a	**6b**
cryst system	monoclinic	triclinic
space group	$P2_1/n$	$P\bar{1}$
a, Å	23.600 (5)	9.121 (4)
b, Å	9.343 (2)	9.964 (3)
c, Å	28.774 (4)	15.729 (4)
α, deg	(90)	85.63 (2)
β, deg	97.39 (2)	83.30 (3)
γ, deg	(90)	85.74 (4)
V, Å^3	6292 (2)	1412.5 (8)
Z	8	2
mol wt	1309.0	1270.9
D(calcd), g cm^{-3}	2.76	2.99
μ, cm^{-1}	167.1	186.1
T, °C	22	23

(B) Measurement of Intensity Data

diffractometer: Syntex P2_1
radiatn: Mo K$\bar{\alpha}$ ($\bar{\lambda}$ = 0.710 730 Å)
monochromator: pyrolytic graphite ($2\theta_{max}$ = 12.2°), equatorial mode; assumed 50% perfect/50% ideally mosaic for polarization correction
reflctns measd: **1a**, 6744 for ±*h*,+*k*,+*l* and 2θ = 4.5–40.0°, yielding 5816 unique data; **6b**, 5355 for +*h*,±*k*,±*l* and 2θ = 4.5–50.0°, yielding 4868 unique data
scan type: coupled θ(crystal)–2θ(counter) at 2.5 deg/min in 2θ
scan range: symmetrical, from [2θ(Kα_1) − Δ]° through [2θ(Kα_2) + Δ]°, Δ = 0.9 for **1a** and 1.0 for **6b**
bkgd: stationary crystal and counter at each end of 2θ scan; each for $^1/_4$ of total scan time
std reflctns: 3 approximately mutually orthogonal reflctns collected before every 97 data points; no significant fluctuations nor decay obsd
absorptn correctn: empirical, by interpolation in 2θ and ϕ between normalized transmissn curves of close-to-axial ψ scans

Conversion of Isomer 6a to 6b. Orange crystals of compound **6a** (ca. 3 mg each) were transferred to two NMR tubes, and toluene-d_8 (0.6 mL) was added to each NMR tube. The tubes were sealed, one under vacuum and the other under one atmosphere of carbon monoxide. Each tube was then heated at 100 °C, while the hydride signals, at δ −21.73 for **6a** and at δ −22.29 for **6b**, were monitored periodically by ^{1}H NMR. Both sets of data followed first-order behavior, and neither deviated significantly from a common plot of ln {[**6a**]/([**6a**] + [**6b**])} vs time, which provided $k = (4.1 \pm 0.2) \times 10^{-5}$ s^{-1}.

Preparation of ^{13}C-Enriched Compounds. Carbon-13 CO-enriched CpWOs$_3$(*CO)$_{12}$H was prepared from ^{13}CO-enriched Os$_3$(*CO)$_{12}$[10] by the reported procedure. This material was utilized to prepare ^{13}CO-enriched CpWOs$_3$(*CO)$_{10}$(μ_3-η^2-C_2Tol_2)H (**1a***) by the procedure described. Compound **2a** enriched with carbon-13 at the alkyne carbon, CpWOs$_3$(CO)$_{10}$(μ_3-η^2-(Ph*CCPh))H (**2a***), was synthesized by using Ph*CCPh (ca. 50% enriched), and this was then used to prepare CpWOs$_3$(CO)$_9$(μ_3-*CPh)$_2$H (**2d***). Compound **1a***: ^{13}C NMR (toluene-d_8, 20 °C) δ 214.6 (s, $^1J_{WC}$ = 175 Hz), 184.5 (s), 181.4 (s), 177.8 (s), 166.5 (d, $^2J_{CH}$ = 10.5 Hz). Compound **2a***: ^{13}C NMR (CD_2Cl_2, 25 °C) δ 143.8 (acetylenic carbon). Compound **2d***: ^{13}C NMR (CD_2Cl_2, 25 °C) δ 268.1 ($^1J_{WC}$ = 106 Hz, alkylidyne carbon).

Collection of X-ray Diffraction Data for CpWOs$_3$(CO)$_{10}$(μ_3-η^2-C_2Tol_2)H (1a). All crystals of this complex gave rather weak diffraction patterns. The crystal selected for the X-ray diffraction study (approximate dimensions 0.1 × 0.15 × 0.2 mm^3) was sealed into a glass capillary and mounted on our Syntex P2_1 automated diffractometer. Subsequent setup operations (i.e., determination of cell parameters and orientation matrix) and collection of the intensity data were carried out as described previously;[11] details appear in Table I. The diffraction

---

[10] Clauss, A. D.; Tachikawa, M.; Shapley, J. R.; Pierpont, C. G. *Inorg. Chem.* **1981**, *20*, 1528.

[11] Churchill, M. R.; Lashewycz, R. A.; Rotella, F. J. *Inorg. Chem.* **1977**, *16*, 265.

Table II. Final Atomic Parameters for $CpWOs_3(CO)_{10}(\mu_3\text{-}\eta^2\text{-}C_2Tol_2)H$ (1a)

atom	*x*	*y*	*z*	*B*, Å^2	atom	*x*	*y*	*z*	*B*, Å^2
				(A) Molecule "A"					
Os(1)	0.32115 (9)	0.28707 (20)	0.34269 (7)		C(10)	0.2595 (22)	−0.005 (5)	0.4457 (17)	2.8 (11)
Os(2)	0.38568 (8)	0.20813 (20)	0.43257 (6)		C(11)	0.4055 (19)	0.062 (4)	0.3783 (14)	1.9 (9)
Os(3)	0.31812 (8)	0.00816 (20)	0.38000 (7)		C(12)	0.3745 (22)	0.098 (5)	0.3332 (17)	3.2 (11)
W	0.25734 (9)	0.19282 (21)	0.42385 (7)		C(13)	0.3874 (18)	0.044 (4)	0.2868 (14)	1.9 (8)
O(1)	0.2356 (16)	0.178 (4)	0.2623 (13)	4.5 (9)	C(14)	0.4031 (24)	0.135 (6)	0.2550 (19)	4.0 (12)
O(2)	0.3791 (16)	0.492 (4)	0.2815 (12)	4.4 (8)	C(15)	0.4243 (23)	0.084 (5)	0.2130 (17)	3.3 (12)
O(3)	0.2464 (18)	0.551 (5)	0.3563 (17)	6.2 (10)	C(16)	0.4204 (21)	−0.065 (5)	0.2038 (17)	8.41 (11)
O(4)	0.5149 (18)	0.250 (4)	0.4535 (13)	5.2 (9)	C(17)	0.3989 (22)	−0.151 (5)	0.2378 (17)	3.1 (11)
O(5)	0.3842 (16)	−0.008 (4)	0.5100 (13)	4.6 (8)	C(18)	0.3847 (20)	−0.100 (5)	0.2784 (16)	2.4 (10)
O(6)	0.3718 (17)	0.472 (4)	0.4937 (14)	5.8 (9)	C(19)	0.4428 (21)	−0.121 (5)	0.1596 (16)	2.7 (10)
O(7)	0.2360 (17)	−0.134 (4)	0.3063 (13)	5.2 (9)	C(20)	0.4565 (20)	−0.024 (5)	0.3810 (16)	2.6 (10)
O(8)	0.3420 (18)	−0.286 (5)	0.4221 (14)	6.1 (10)	C(21)	0.5021 (23)	0.003 (5)	0.3510 (18)	3.4 (11)
O(9)	0.1638 (16)	0.108 (4)	0.3415 (12)	3.7 (8)	C(22)	0.5520 (23)	−0.077 (6)	0.3588 (18)	3.7 (12)
O(10)	0.2479 (17)	−0.109 (4)	0.4661 (13)	5.1 (9)	C(23)	0.5620 (24)	−0.179 (6)	0.3902 (19)	3.9 (12)
C(1)	0.2694 (23)	0.231 (4)	0.2930 (17)	2.7 (10)	C(24)	0.5193 (22)	−0.207 (5)	0.4201 (17)	3.2 (11)
C(2)	0.3574 (21)	0.412 (5)	0.3047 (16)	2.5 (10)	C(25)	0.4693 (19)	−0.126 (5)	0.4162 (15)	2.1 (9)
C(3)	0.2757 (23)	0.447 (5)	0.3533 (17)	3.7 (11)	C(26)	0.6180 (25)	−0.267 (6)	0.3950 (20)	4.5 (13)
C(4)	0.4674 (19)	0.235 (4)	0.4442 (14)	1.9 (8)	C(27)	0.1730 (24)	0.244 (6)	0.4523 (19)	4.2 (12)
C(5)	0.3871 (21)	0.068 (5)	0.4815 (17)	2.8 (10)	C(28)	0.2129 (22)	0.214 (5)	0.4920 (17)	3.3 (11)
C(6)	0.3738 (21)	0.378 (5)	0.4726 (16)	2.6 (10)	C(29)	0.2554 (26)	0.318 (6)	0.4933 (20)	4.8 (14)
C(7)	0.2687 (22)	−0.082 (5)	0.3348 (17)	3.0 (11)	C(30)	0.2466 (22)	0.422 (5)	0.4582 (17)	4.0 (11)
C(8)	0.3349 (27)	−0.166 (7)	0.4038 (21)	4.9 (14)	C(31)	0.1930 (24)	0.373 (6)	0.4300 (18)	4.4 (12)
C(9)	0.1986 (21)	0.134 (5)	0.3711 (17)	2.3 (10)					
				(B) Molecule "B"					
Os(1)	0.86163 (8)	0.32349 (19)	0.31629 (6)		C(10)	0.7621 (21)	0.039 (5)	0.3987 (16)	2.9 (10)
Os(2)	0.89696 (8)	0.24033 (20)	0.41295 (7)		C(11)	0.9293 (18)	0.090 (4)	0.3631 (14)	1.5 (9)
Os(3)	0.84138 (8)	0.04605 (20)	0.34924 (6)		C(12)	0.9131 (20)	0.135 (5)	0.3174 (16)	2.3 (10)
W	0.76839 (9)	0.23307 (22)	0.37687 (7)		C(13)	0.9354 (20)	0.075 (5)	0.2768 (15)	2.9 (10)
O(1)	0.8099 (17)	0.250 (4)	0.2177 (14)	5.2 (9)	C(14)	0.9282 (20)	−0.073 (5)	0.2650 (16)	2.2 (10)
O(2)	0.9387 (18)	0.529 (4)	0.2738 (14)	5.8 (10)	C(15)	0.9501 (21)	−0.125 (5)	0.2268 (17)	3.2 (11)
O(3)	0.7874 (15)	0.599 (4)	0.3195 (12)	4.4 (8)	C(16)	0.9747 (21)	−0.036 (5)	0.1946 (16)	3.0 (10)
O(4)	1.0214 (20)	0.285 (5)	0.4480 (15)	6.1 (10)	C(17)	0.9815 (20)	0.105 (5)	0.2070 (15)	2.7 (10)
O(5)	0.8744 (15)	0.028 (4)	0.4896 (12)	4.2 (8)	C(18)	0.9616 (19)	0.161 (4)	0.2465 (15)	2.9 (9)
O(6)	0.8655 (16)	0.502 (4)	0.4681 (13)	4.7 (9)	C(19)	0.9925 (23)	−0.096 (6)	0.1472 (18)	3.9 (12)
O(7)	0.7906 (15)	−0.080 (4)	0.2565 (12)	3.9 (8)	C(20)	0.9774 (21)	−0.012 (4)	0.3790 (16)	3.0 (10)
O(8)	0.8497 (19)	−0.240 (5)	0.3979 (15)	6.6 (11)	C(21)	0.9784 (23)	−0.104 (6)	0.4185 (17)	4.0 (11)
O(9)	0.6951 (14)	0.1250 (34)	0.2838 (11)	3.5 (7)	C(22)	1.0241 (25)	−0.201 (6)	0.4309 (19)	4.9 (13)
O(10)	0.7433 (18)	−0.069 (5)	0.4137 (14)	5.9 (10)	C(23)	1.0736 (22)	−0.202 (5)	0.4069 (17)	3.7 (11)
C(1)	0.8249 (22)	0.278 (5)	0.2540 (18)	3.0 (11)	C(24)	1.0719 (24)	−0.107 (6)	0.3712 (19)	4.5 (13)
C(2)	0.9117 (24)	0.449 (6)	0.2913 (18)	3.7 (12)	C(25)	1.0266 (21)	−0.014 (5)	0.3540 (16)	3.2 (10)
C(3)	0.8112 (23)	0.491 (6)	0.3204 (18)	4.5 (12)	C(26)	1.1239 (25)	−0.306 (6)	0.4263 (19)	5.0 (13)
C(4)	0.9737 (22)	0.272 (5)	0.4348 (16)	2.7 (10)	C(27)	0.6715 (24)	0.302 (6)	0.3827 (18)	3.9 (12)
C(5)	0.8851 (21)	0.108 (5)	0.4631 (17)	3.0 (11)	C(28)	0.7033 (24)	0.411 (6)	0.3682 (18)	3.6 (12)
C(6)	0.8732 (22)	0.402 (6)	0.4465 (17)	3.4 (11)	C(29)	0.7460 (25)	0.461 (6)	0.4059 (19)	4.7 (13)
C(7)	0.8106 (20)	−0.038 (5)	0.2911 (16)	2.6 (10)	C(30)	0.7478 (26)	0.350 (6)	0.4455 (20)	4.3 (14)
C(8)	0.8479 (24)	−0.127 (6)	0.3765 (18)	4.4 (12)	C(31)	0.7011 (26)	0.254 (6)	0.4313 (20)	5.3 (13)
C(9)	0.7273 (22)	0.164 (5)	0.3190 (17)	3.3 (11)					

symmetry ($2/m$; C_{2h}) and systematic absences ($h0l$ for $h + l = 2n + 1$ and $0k0$ for $k = 2n + 1$) uniquely define the centrosymmetric monoclinic space group $P2_1/n$. Data collection was terminated at $2\theta = 40.0°$ (Mo Kα), since there were few observable relfections beyond this angle. All data were corrected for the effects of absorption and for Lorentz and polarization factors, were converted to unscaled $|F_o|$ values, and were placed on an approximately absolute scale by means of a Wilson plot. Any reflection with $I(\text{net}) < 0$ was assigned the value $|F_o| = 0$. No data were rejected.

Solution and Refinement of the Structure of $CpWOs_3(CO)_{10}(\mu_3\text{-}\eta^2\text{-}C_2Tol_2)H$ (1a). All calculations were performed on our locally modified version of the Syntex XTL system. The analytical form of the appropriate neutral atom scattering factor was used and was corrected for both the real ($\Delta f'$) and imaginary ($i\Delta f''$) components of anomalous dispersion.[12] The function minimized during full-matrix least-squares refinement was $\sum w(|F_o| - |F_c|)^2$, where $w = [(\sigma|F_o|)^2 + (0.015|F_o|)^2]^{-1}$.

The eight heavy atoms were located by using MULTAN.[13] All non-hydrogen atoms were found on subsequent difference Fourier maps. Discrepancy indices used below are defined in eq 1–3. Here, NO = number of observations and NV = number of variables.

$$R_F\,(\%) = 100\,\sum||F_o| - |F_c||/\sum|F_o| \tag{1}$$

$$R_{wF}\,(\%) = 100[\sum w(|F_o| - |F_c|)^2/\sum w|F_o|^2]^{1/2} \tag{2}$$

$$\text{GOF} = [\sum w(|F_o| - |F_c|)^2/(\text{NO} - \text{NV})]^{1/2} \tag{3}$$

Following a minor correction for the effects of secondary extinction ($g = 2.54 \times 10^{-7}$) using the approximation to the Zachariasen correction shown in eq 4, refinement (anisotropic for

$$|F_{o,\text{corr}}| = (1.0 + gI_o)|F_{o,\text{uncor}}| \tag{4}$$

heavy metals; isotropic for all others) converged with $R_F = 8.6\%$, $R_{wF} = 7.6\%$, and GOF = 1.18 for 409 parameters refined against all 5816 reflections. Discrepancy indices for those 4223 reflections with $|F_o| > 3.0\sigma(|F_o|)$ were $R_F = 5.0\%$ and $R_{wF} = 6.3\%$; the substantially lower values for the latter set are simply an indication of the large number of very weak (and inherently imprecise) data obatined from the weakly diffracting crystal.

A final difference Fourier synthesis showed a number of peaks of height ~1.0–1.5 e/Å^3 in the vicinity of the heavy atoms. Hydride ligands could not be located with any certainty and were not included in the model (however, see discussion); hydrogen atoms in the organic fragments also were not included, due to

---

(12) *International Tables for X-Ray Crystallography*; Kynoch: Birmingham, England 1974; Vol. 4, pp 99–101, 149–150.

(13) Germain, G.; Main, P.; Woolfson, M. M. *Acta Crystallogr., Sec. A: Cryst. Phys., Diffr., Theor. Gen. Crystallogr.* **1971**, *A27*, 368.

Table III. Final Atomic Parameters for $CpWOs_3(CO)_{10}(\mu_3\text{-}\eta^2\text{-}C_2(CO_2Et)_2)H$ (6b)

atom	x	y	z
Os(1)	0.69248 (5)	0.88969 (5)	0.17018 (3)
Os(2)	0.37917 (6)	0.88221 (5)	0.22651 (3)
Os(3)	0.58982 (6)	0.86733 (5)	0.35122 (3)
W	0.54193 (6)	0.65129 (5)	0.24824 (3)
O(1)	0.7677 (17)	0.6036 (13)	0.4556 (7)
O(2)	0.8779 (14)	0.4951 (10)	0.3457 (7)
O(3)	1.0300 (11)	0.6590 (10)	0.1813 (8)
O(4)	0.8832 (11)	0.5052 (9)	0.1552 (7)
O(11)	1.0093 (13)	0.9665 (12)	0.1273 (11)
O(12)	0.6674 (19)	0.8557 (13)	−0.0173 (7)
O(13)	0.5857 (12)	1.1852 (9)	0.1335 (8)
O(21)	0.1055 (14)	0.8115 (15)	0.3411 (9)
O(22)	0.2568 (14)	1.1743 (11)	0.2065 (8)
O(23)	0.2825 (15)	0.7991 (13)	0.0614 (7)
O(31)	0.4241 (16)	1.1489 (9)	0.3703 (7)
O(32)	0.8222 (16)	0.9201 (15)	0.4668 (8)
O(33)	0.3904 (16)	0.7437 (13)	0.4996 (7)
O(41)	0.6129 (17)	0.5798 (13)	0.0546 (8)
C(11)	0.8949 (18)	0.9350 (16)	0.1435 (11)
C(12)	0.6750 (18)	0.8616 (14)	0.0539 (10)
C(13)	0.6143 (14)	1.0688 (12)	0.1481 (8)
C(21)	0.2042 (18)	0.8397 (17)	0.2968 (10)
C(22)	0.3111 (16)	1.0687 (14)	0.2128 (9)
C(23)	0.3185 (15)	0.8344 (15)	0.1233 (9)
C(31)	0.4827 (20)	1.0399 (16)	0.3610 (9)
C(32)	0.7366 (21)	0.8999 (15)	0.4239 (10)
C(33)	0.4622 (20)	0.7886 (16)	0.4450 (9)
C(41)	0.5847 (19)	0.6083 (14)	0.1272 (10)
C(1)	0.7892 (17)	0.5915 (14)	0.3823 (9)
C(2)	0.7267 (16)	0.6919 (12)	0.3133 (9)
C(3)	0.7747 (13)	0.6973 (10)	0.2254 (8)
C(4)	0.9076 (15)	0.6189 (12)	0.1862 (9)
C(5)	0.9514 (27)	0.3966 (20)	0.4014 (14)
C(6)	0.9928 (50)	0.2796 (32)	0.3601 (21)
C(7)	1.0085 (19)	0.4252 (14)	0.1178 (12)
C(8)	0.9564 (26)	0.3084 (20)	0.0875 (16)
Cp(1)	0.5466 (26)	0.4220 (20)	0.2769 (14)
Cp(2)	0.4958 (24)	0.4826 (18)	0.3555 (12)
Cp(3)	0.3605 (24)	0.5482 (19)	0.3471 (13)
Cp(4)	0.3183 (21)	0.5287 (17)	0.2669 (11)
Cp(5)	0.4364 (23)	0.4505 (17)	0.2268 (12)
H(12)	0.578 (16)	0.936 (12)	0.249 (8)

limitations in the computer core. Final positional parameters are presented in Table II.

Collection of X-ray Diffraction Data for $CpWOs_3(CO)_{10}(\mu_3\text{-}\eta^2\text{-}C_2(CO_2Et)_2)H$ (6b). The crystal selected for the X-ray study was a well-formed parallelepiped of approximate dimensions 0.1 × 0.1 × 0.15 mm^3. It was mounted, in air, on a glass fiber. Data collection etc. was similar to that for **1a** unless otherwise state; details are presented in Table I. The crystal showed no diffraction symmetry other than the Friedel condition ($\bar{1}$, C_i) and is therefore triclinic. Possible space groups are $P1$ (No. 1) or $P\bar{1}$ (No. 2). The latter was chosen on the basis of cell volume (V = 1412.5 (8) Å^3, consistent with Z = 2) and the documented greater probability of a synthetic material crystallizing in a centrosymmetric space group (particularly $P\bar{1}$ vs $P1$ with Z = 2).[14] Data were collected out to 2θ = 50° (Mo Kα), since the crystal quality and diffracting qualities were far better than for **1a**.

Solution and Refinement of the Crystal Structure of $CpWOs_3(CO)_{10}(\mu_3\text{-}\eta^2\text{-}C_2(CO_2Et)_2)H$ (6b). Attempts to solve the structure using MULTAN on the Syntex XTL system were unsuccessful. It was subsequently solved by using the SHELX-76 direct methods program of G. M. Sheldrick on the CDC Cyber 173 computer at the Computer Center at SUNY—Buffalo. All non-hydrogen atoms were located and refined with anisotropic thermal parameters. The apparent location of the hydride ligand was determined from a difference Fourier synthesis and convergence was reached with R_F = 5.55% and R_{wF} = 5.89% for 404 parameters refined against 4868 data (R_F = 4.87%, R_{wF} = 5.18% for those 4240 data with $|F_o| > 3\sigma(|F_o|)$). A final difference Fourier synthesis was featureless apart from residual peaks (~1.1 e/Å^3) close to the positions of the metal atoms. Final positional parameters are collected in Table III.

Note that, both in this structural study and in the previous one, the identity of W vs Os rests, principally, on its being connected to the Cp ligand. With Z(W) = 74 and Z(Os) = 76 it is not possible to distinguish unambiguously between these atom types on the basis of occupacy refinement etc.

Table IV. Isolated Yields of Various Tungsten-Triosmium Alkyne Complexes

alkyne (RC_2R')	yield (%) a	yield (%) b	reactn time (h)
R = R′ = Tol	48 (**1a**)	0	1
R = R′ = Ph	45 (**2a**)	0	1
R = Ph R′ = Tol	42 (**3a**)	0	1
R = R′ = H[a]	30 (**4a**)	0	0.5
R = Ph R′ = CO_2Et	17 (**5a**)	33 (**5b**/**5c**)[b]	1
R = R′ = CO_2Et	26 (**6a**)	23 (**6b**)	0.5
R = R′ = CF_3	7 (**7a**)	38 (**7b**)	0.5

[a] Data from ref 4b. [b] A mixture of two isomers (5:2).

Results and Discussion

Preparation and Characterization of Isomeric $CpWOs_3(CO)_{10}(\mu_3\text{-}\eta^2\text{-}C_2RR')H$. The complex $CpWOs_3(CO)_{12}H$ reacts with various alkynes in refluxing toluene to give a series of isomeric $CpWOs_3(CO)_{10}(\mu_3\text{-}\eta^2\text{-}C_2RR')H$ clusters according to eq 5. Better yields have been obtained by initial decarbonylation with Me_3NO/MeCN followed by pyrolysis in refluxing toluene.

$$CpWOs_3(CO)_{12}H + C_2RR' \xrightarrow[-2CO]{\Delta} CpWOs_3(CO)_{10}(C_2RR')H \quad (5)$$

Two isomers of $CpWOs_3(CO)_{10}(C_2RR')H$, symmetrical (isomer **a**) and unsymmetrical (isomer **b**), are formed, depending on the substituents R and R′ of an alkyne. The structures of the two isomers, as indicated by the spectroscopic and crystallographic results, are shown.

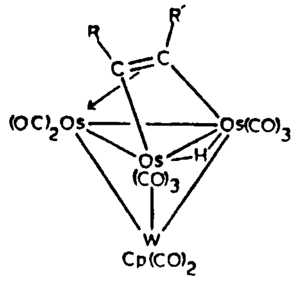

a

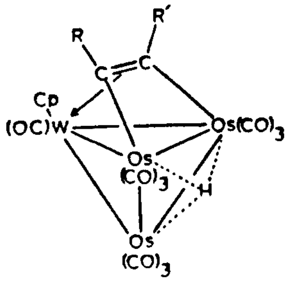

b

1a: R = R′ = Tol
2a: R = R′ = Ph
3a: R = Ph; R′ = Tol
4a: R = R′ = H
5a: R = Ph; R′ = CO_2Et
6a: R = R′ = CO_2Et
7a: R = R′ = CF_3

5b/**5c**: R = Ph;
R′ = CO_2Et/R = CO_2Et;
R′ = Ph
6b: R = R′ = CO_2Et
7b: R = R′ = CF_3

The various alkynes used, yield data, and reaction times are shown in Table IV. With the top four alkynes (R = H or aryl) only a symmetrical isomer (**a**) is obtained, while both symmetrical (**a**) and unsymmetrical (**b**) isomers are isolated with the bottom three alkynes (R = CO_2Et or CF_3). The reaction with $PhC{\equiv}CCO_2Et$ yields a symmetrical isomer **5a** and a mixture of two unsymmetrical isomers **5b** and **5c** (in a ratio of 5:2). Except for the **5b**/**5c** mixture, all these isomers are readily separated either by prepara-

---

(14) Nowacki, W.; Matsumoto, T.; Edenharter, A. *Acta Crystallogr.* **1967**, *22*, 935.

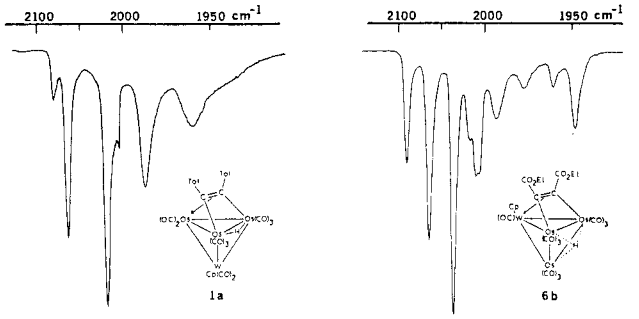

Figure 1. Infrared spectra (carbonyl region) of **1a** and **6b**.

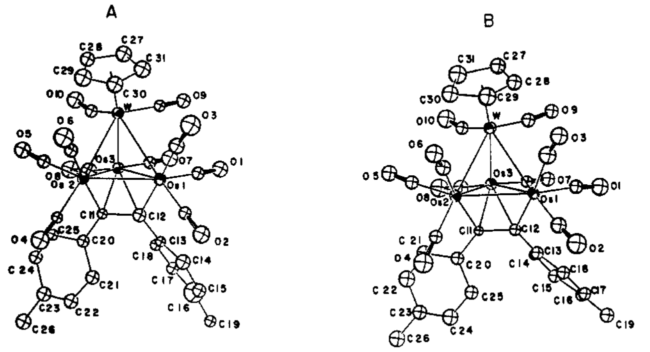

Figure 2. Labeling of atoms and molecular connectivity for the two independent molecules of $CpWOs_3(CO)_{10}(\mu_3\text{-}\eta^2\text{-}C_2Tol_2)H$ (**1a**). Note the approximate vertical mirror plane.

tive TLC on silica gel or by fractional recrystallization.

The formulations for compounds **1a**–**7b** were established by spectroscopic and analytical data. The ^1H NMR spectra of the symmetrical isomers **1a**, **2a**, and **6a** reveal that both substituents R_2 are equivalent. The ^{19}F NMR spectrum of **7a** likewise shows a single resonance for both CF_3 groups. With the compounds **6b** and **7b**, two distinct groups of resonances are observed for R_2 in the ^1H and ^{19}F NMR spectra, respectively, indicating their unsymmetrical structures.

The carbonyl regions of the IR spectra for **1a** and **6b** are shown in Figure 1 and are representative of all the derivatives. The IR spectra of the symmetrical isomers, **1a**–**7a**, are identical except that an extra band is observed for compounds **3a** and **5a**, in which R and R′ substituents are different (**3a**, 2013 cm^{-1}; **5a**, 2018 cm^{-1}). Likewise, the spectra of the **5b**/**5c** mixture as well as **6b** and **7b** are quite similar; each cluster shows three characteristic intense bands in the 2100–2030 cm^{-1} region. The close similarities of the IR spectra indicate likely structural correspondence in the various isomeric alkyne clusters.

Description of the Structure of $CpWOs(CO)_{10}(\mu_3\text{-}\eta^2\text{-}C_2Tol_2)H$ (1a). A brief account of this structure has appeared previously.[4a]

The crystal consists of discrete molecular units that are mutually separated by normal van der Waals' contacts; there are no abnormally short intermolecular contacts. The crystallographic asymmetric unit contains two entire molecules, referred to hereafter as molecules "A" and "B". The two molecules are essentially equivalent both in terms of connectivity and ligand conformation. As shown in Figure 2, the solid-state structure has close to $C_s(m)$ symmetry except for (a) an offset of the Cp ligand from a truly symmetrical capping position on tungsten, (b) the clearly related phenomenon of C(10)–O(10) having "semibridging" properties[15] in contrast to C(9)–O(9) being strictly terminal, and (c) noncorrespondence of the *p*-tolyl groups caused by different rotomeric conformations about the C(11)–C(20) and C(12)–C(13) bonds.

Table V. Interatomic Distances (Å) for $CpWOs_3(CO)_{10}(\mu_3\text{-}\eta^2\text{-}C_2Tol_2)H$ (1a)

	molecule A	molecule B
(A) Metal–Metal Distances		
W–Os(1)	3.066 (3)	3.095 (3)
W–Os(2)	3.010 (3)	3.079 (3)
W–Os(3)	2.663 (3)	2.647 (3)
Os(1)–Os(2)	2.922 (3)	2.905 (3)
Os(1)–Os(3)	2.823 (3)	2.822 (3)
Os(2)–Os(3)	2.775 (3)	2.785 (3)
(B) Metal–Carbonyl Distances		
Os(1)–C(1)	1.83 (5)	1.94 (5)
Os(1)–C(2)	1.88 (5)	1.87 (6)
Os(1)–C(3)	1.89 (5)	1.98 (6)
Os(2)–C(4)	1.93 (5)	1.86 (5)
Os(2)–C(5)	1.92 (5)	1.95 (5)
Os(2)–C(6)	2.00 (5)	1.91 (5)
Os(3)–C(7)	1.84 (5)	1.90 (5)
Os(3)–C(8)	1.79 (6)	1.79 (6)
W–C(9)	2.00 (5)	1.93 (5)
W–C(10)	1.95 (5)	1.93 (5)
Os(3)···C(10)	2.48 (5)	2.49 (5)
(C) Metal–Carbon (μ_3-η^2-Alkyne) Distances		
Os(2)–C(11)	2.17 (4)	2.21 (4)
Os(3)–C(11)	2.13 (4)	2.10 (3)
Os(1)–C(12)	2.21 (5)	2.14 (5)
Os(3)–C(12)	2.18 (5)	2.19 (5)
Os(3)···midpt[a]	2.03	2.03
(D) Carbon–Oxygen Distances		
C(1)–O(1)	1.22 (6)	1.09 (6)
C(2)–O(2)	1.17 (6)	1.14 (7)
C(3)–O(3)	1.21 (7)	1.15 (7)
C(4)–O(4)	1.13 (6)	1.15 (7)
C(5)–O(5)	1.10 (6)	1.12 (6)
C(6)–O(6)	1.08 (6)	1.15 (6)
C(7)–O(7)	1.15 (6)	1.12 (6)
C(8)–O(8)	1.24 (7)	1.22 (7)
C(9)–O(9)	1.13 (6)	1.24 (6)
C(10)–O(10)	1.19 (6)	1.21 (6)
(E) Tungsten–Carbon (Cp) Distances		
W–C(27)	2.30 (6)	2.40 (6)
W–C(28)	2.35 (5)	2.26 (6)
W–C(29)	2.32 (6)	2.37 (6)
W–C(30)	2.39 (5)	2.36 (6)
W–C(31)	2.29 (66)	2.38 (6)
W···centroid	1.99	2.00
(F) Acetylenic C–C Distance within the C_2Tol_2 Ligand		
C(11)–C(12)	1.45 (6)	1.38 (6)

[a] Midpt = midpoint.

Bond distances and angles are listed in Tables V and VI in such a fashion that equivalent values for molecules A and B appear side by side. In subsequent discussions distances and angles will be given with the value for molecule A first, followed by that for molecule B.

The WOs_3 system defines a tetrahedron. The cluster as a whole is, as expected for a tetrahedral arrangement, associated with 60 outer valence electrons. The lengthened Os(1)–Os(2) bond (2.922 (3) and 2.905 (3) Å as compared to Os(1)–Os(3) = 2.823 (3) and 2.822 (3) Å and Os(2)–Os(3) = 2.775 (3) and 2.785 (3) Å) suggests that this bond is associated with the bridging hydride ligand (possibly in that location trans to both C(1)–O(1) and C(5)–O(5)). Os(1) and Os(2) each bear three terminal carbonyl ligands, whereas Os(3) and W each have only two. The μ_3-η^2-C_2Tol_2 ligand lies on the Os_3 face of the WOs_3 cluster and is formally π-bonded to Os(3) (Os(3)–C(11) = 2.13 (4) and 2.10 (3) Å, Os(3)–C(12) = 2.18 (5) and 2.19 (5) Å, Os(3)···midpoint = 2.03 and 2.03 Å) and σ-bonded to Os(1) and

---

[15] Cotton, F. A. *Prog. Inorg. Chem.* **1976**, *21*, 1.

Table VI. Selected Interatomic Angles (deg) for CpWOs$_3$(CO)$_{10}$(μ_3-η^2-C$_2$Tol$_2$)H (1a)

	molecule A	molecule B		molecule A	molecule B
(A) Intermetallic Angles					
Os(2)–Os(1)–Os(3)	57.74 (7)	58.18 (7)	Os(1)–Os(3)–Os(2)	62.92 (7)	62.40 (7)
Os(2)–Os(1)–W	60.30 (7)	61.64 (6)	Os(1)–Os(3)–W	67.89 (7)	68.86 (7)
Os(3)–Os(1)–W	53.58 (6)	52.89 (6)	Os(2)–Os(3)–W	67.19 (7)	69.00 (7)
Os(1)–Os(2)–Os(3)	59.34 (7)	59.42 (7)	Os(1)–W–Os(2)	57.47 (6)	56.13 (6)
Os(1)–Os(2)–W	62.22 (7)	62.22 (7)	Os(1)–W–Os(3)	58.53 (7)	58.25 (7)
Os(3)–Os(2)–W	54.63 (7)	53.37 (6)	Os(2)–W–Os(3)	58.18 (7)	57.63 (7)
(B) M–M–CO and Os–W–Cp Angles					
Os(2)–Os(1)–C(1)	146.9 (15)	150.1 (15)	Os(1)–Os(3)–C(7)	101.7 (16)	98.3 (14)
–C(2)	116.6 (15)	114.7 (17)	–C(8)	165.8 (20)	164.9 (18)
–C(3)	107.4 (16)	104.8 (16)	Os(2)–Os(3)–C(7)	164.6 (16)	160.1 (14)
Os(3)–Os(1)–C(1)	89.2 (15)	91.9 (15)	–C(8)	108.6 (20)	107.0 (18)
–C(2)	146.1 (15)	147.8 (17)	W–Os(3)–C(7)	107.6 (16)	110.3 (14)
–C(3)	128.8 (16)	125.3 (16)	–C(8)	120.9 (20)	119.1 (18)
W–Os(1)–C(1)	99.7 (15)	101.3 (15)	Os(1)–W–C(9)	82.0 (14)	85.4 (15)
–C(2)	158.0 (15)	156.5 (17)	–C(10)	121.5 (15)	122.0 (14)
–C(3)	76.0 (15)	72.9 (16)	Os(2)–W–C(9)	132.0 (14)	131.6 (15)
Os(1)–Os(2)–C(4)	121.1 (13)	115.2 (15)	–C(10)	91.9 (15)	91.4 (14)
–C(5)	141.3 (14)	146.0 (15)	Os(3)–W–C(9)	79.9 (14)	78.2 (15)
–C(6)	102.4 (14)	101.9 (15)	–C(10)	62.9 (15)	63.8 (14)
Os(3)–Os(2)–C(4)	132.3 (13)	133.0 (15)	Os(1)–W–Cp	128.1	129.0
–C(5)	84.1 (14)	88.5 (15)	Os(2)–W–Cp	119.2	120.2
–C(6)	137.3 (14)	134.6 (15)	Os(3)–W–Cp	171.5	171.1
W–Os(2)–C(4)	173.0 (13)	172.0 (15)	Os(1)–Os(3)···C(10)	112.3 (12)	112.9 (11)
–C(5)	87.2 (14)	90.4 (15)	Os(2)–Os(3)···C(10)	87.5 (12)	88.1 (11)
–C(6)	82.6 (14)	81.2 (15)	W–Os(3)–C(10)	44.4 (12)	44.0 (11)
(C) M–C–O Angles					
Os(1)–C(1)–O(1)	172.5 (41)	172.6 (47)	Os(3)–C(7)–O(7)	176.7 (45)	176.2 (42)
–C(2)–O(2)	178.4 (43)	174.8 (48)	–C(8)–O(8)	174.3 (52)	174.5 (48)
–C(3)–O(3)	174.7 (45)	170.4 (46)	W–C(9)–O(9)	175.9 (42)	172.5 (41)
Os(2)–C(4)–O(4)	176.4 (40)	176.8 (45)	W–C(10)–O(10)	159.7 (42)	162.1 (41)
–C(5)–O(5)	175.0 (44)	174.1 (44)	Os(3)···C(10)–O(10)	127.2 (37)	124.2 (36)
–C(6)–O(6)	174.2 (46)	172.1 (45)	W–C(10)···Os(3)	72.7 (16)	72.2 (15)
(D) M–C(Alkyne)–M Angles					
Os(2)–C(11)–Os(3)	80.4 (15)	80.4 (14)	Os(1)–C(12)–Os(3)	80.2 (17)	81.4 (16)
(E) M–C–C Angles Associated with the Alkyne Ligand					
Os(2)–C(11)–C(12)	111.6 (31)	110.5 (30)	Os(1)–C(12)–C(11)	107.9 (32)	110.4 (31)
Os(3)–C(11)–C(12)	72.3 (26)	74.5 (26)	Os(3)–C(12)–C(11)	68.5 (26)	67.9 (25)
Os(2)–C(11)–C(20)	124.6 (31)	121.0 (29)	Os(1)–C(12)–C(13)	124.6 (33)	124.5 (33)
Os(3)–C(11)–C(20)	132.1 (32)	128.2 (29)	Os(3)–C(12)–C(13)	129.1 (33)	124.9 (33)
(F) Carbon–Metal–Carbon Angles					
C(1)–Os(1)–C(2)	91.8 (21)	90.6 (22)	C(4)–Os(2)–C(6)	90.5 (19)	92.2 (21)
C(1)–Os(1)–C(3)	90.9 (22)	91.7 (22)	C(5)–Os(2)–C(6)	96.1 (20)	92.7 (21)
C(2)–Os(1)–C(3)	85.1 (22)	86.8 (23)	C(7)–Os(3)–C(8)	86.6 (25)	90.9 (23)
C(4)–Os(2)–C(5)	92.1 (19)	94.5 (21)	C(9)–W–C(10)	88.2 (20)	85.2 (21)
(G) C(alkyne)–M–C(carbonyl) Angles					
C(12)–Os(1)–C(1)	90.5 (20)	91.0 (20)	C(11)–Os(3)–C(7)	128.4 (20)	120.2 (18)
–C(2)	96.6 (20)	97.8 (21)	–C(8)	93.2 (23)	93.8 (21)
–C(3)	177.8 (21)	174.7 (20)	···C(10)	131.7 (16)	133.8 (16)
C(11)–Os(2)–C(4)	84.5 (17)	85.3 (18)	C(12)–Os(3)–C(7)	97.1 (21)	90.9 (19)
–C(5)	96.7 (18)	100.0 (18)	–C(8)	117.7 (24)	119.7 (21)
–C(6)	166.4 (18)	167.3 (19)	···C(10)	158.9 (18)	158.0 (16)
(H) Acetylenic C–C–C Angles within the μ_3-C$_2$Tol$_2$ Ligand					
C(11)–C(12)–C(13)	125.7 (42)	124.5 (41)	C(12)–C(11)–C(20)	120.1 (40)	125.6 (39)

Os(2) (Os(1)–C(12) = 2.21 (5) and 2.14 (5) Å, Os(2)–C(11) = 2.17 (4) and 2.21 (4) Å).

Formal electron counts at the individual metal atoms (neutral ligands and metals assumed) are $18^1/_2$e at Os(1) and Os(2), 18e at W, and 17e at Os(3). The electron deficiency at Os(3) apparently is compensated for by *direct* donation of electron density from the tungsten atom. This possibility is indicated by the very short W–Os(3) bond (i.e., W–Os(3) = 2.663 (3) and 2.647 (3) Å as compared to W–Os(1) = 3.066 (3) and 3.095 (3) Å and W–Os(2) = 3.010 (3) and 3.079 (3) Å). In addition, this donor–acceptor interaction is supported by a "semibridging" carbonyl group in a typical fashion.[15]

The TolC≡CTol ligand is bent with ∠C(12)–C(11)–C(20) = 120.1 (40) and 125.6 (39)° and ∠C(11)–C(12)–C(13) = 125.7 (42) and 124.5 (41)° (average = 123.9 ± 2.4°), and the original triple bond is now lengthened to C(11)–C(12) = 1.45 (6) and 1.38 (6) Å.

All other distances and angles are in the expected ranges but are of relatively low accuracy because of poor crystal quality. Thus Os–CO = 1.79 (6)–2.00 (5) Å (average = 1.89 ± 0.06Å), W–CO = 1.93 (5)–2.00 (5) Å (average = 1.95 ± 0.03 Å), and C–O = 1.08 (6)–1.24 (6) Å (average = 1.16 ± 0.05 Å). All M–C–O angles are close to 180° (range = 170.4 (46)–178.4 (43) Å) other than that associated with the "semibridging" carbonyl group. Geometric parameters pertinent to this unique ligand are as follows: W–C(10) = 1.95 (5) and 1.93 (5) Å, Os(3)···C(10) = 2.48 (5) and 2.49 (5) Å, ∠W–C(10)–O(10) = 159.7 (42) and 162.1 (41)°, ∠Os(3)···C(10)–O(10) = 127.2 (37) and 124.2 (36)°, and

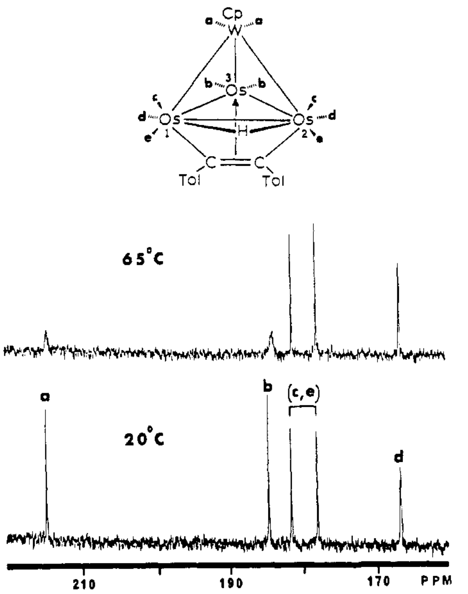

Figure 3. ^{13}C (^1H coupled) NMR spectra (90 MHz) of $CpWOs_3(^*CO)_{10}(\mu_3\text{-}\eta^2\text{-}C_2Tol_2)H$ (**1a***) in toluene-d_8.

∠W–C(10···Os(3) = 72.7 (16) and 72.2 (15)°.

^{13}C NMR Spectra for 1a. Solution ^{13}C NMR data (see Figure 3) for **1a** are fully explicable on the basis of the solid-state structure. Between −70 and +25 °C, the ^{13}C NMR spectrum of $CpWOs_3(CO)_{10}(\mu_3\text{-}\eta^2\text{-}C_2Tol_2)H$ exhibits five equally intense resonances at δ 214.6, 184.5, 181.4, 177.8, and 166.5, implying that the ten carbonyl ligands are pairwise equivalent. The signal at δ 214.6 is assigned to the pair of carbonyl ligands on the tungsten atom (a) on the basis of chemical shift and ^{183}W satellites ($^1J_{WC}$ = 175 Hz). The interconversion of these two carbonyls (one terminal and one semibridging) is apparently sufficiently rapid as to generate an effective plane of symmetry for **1a** in solution. The d pair, positioned trans to the bridging hydrogen, corresponds to the doublet at δ 166.5 with $^2J_{CH}$ = 10.5 Hz; this coupling was verified by obtaining the ^1H-decoupled spectrum. Note that this position for the hydride ligand is consonant with the crystallographic implication that it bridges Os(1)–Os(2).

Increasing the temperature from 20 to 65 °C causes the two resonances at δ 214.6 and 184.5 to broaden to the same extent, while the rest of signals remain sharp. These changes are attributed to carbonyl ligand exchange between the W and Os(3) centers. This is an unusual feature, since the WOs_3 clusters examined previously show carbonyl ligand exchange occurring only in a localized fashion.[1b,16] The internuclear exchange in **1a** is presumably related to both the semibridging carbonyl ligand and the short W–Os(3) bond length (ca. 0.3–0.4 Å shorter than the other W–Os bonds). The resonance at δ 184.5 is, therefore, assigned to the b pair. The Os(1) and Os(2) centers do not undergo observable localized threefold exchange of their carbonyl ligands up to 65 °C. The remaining resonances at δ 181.4 and 177.8 are assigned to the c and e pairs.

Description of the Structure of $CpWOs_3(CO)_{10}(\mu_3\text{-}\eta^2\text{-}C_2(CO_2Et)_2)H$ (6b). The complex crystallizes as an ordered racemic mixture of chiral molecules in the centrosymmetric space group $P\bar{1}$; there are no unusually short intermolecular contacts. The molecular geometry and atomic labeling is shown in Figure 4; interatomic distances and angles are collected in Table VII and VIII, respectively.

Table VII. Interatomic Distances (Å) for $CpWOs_3(CO)_{10}(\mu_3\text{-}\eta^2\text{-}C_2(CO_2Et)_2H$ (6b)

(A) Metal–Metal Distances			
W–Os(1)	2.947 (1)	Os(1)–Os(2)	2.896 (1)
W–Os(2)	2.665 (1)	Os(1)–Os(3)	2.889 (1)
W–Os(3)	2.878 (1)	Os(2)–Os(3)	2.890 (1)
(B) Metal–Carbonyl and C–O Distances			
Os(1)–C(11)	1.924 (17)	C(11)–O(11)	1.108 (20)
Os(1)–C(12)	1.898 (16)	C(12)–O(12)	1.137 (19)
Os(1)–C(13)	1.894 (12)	C(13)–O(13)	1.181 (15)
Os(2)–C(21)	1.888 (16)	C(21)–O(21)	1.112 (20)
Os(2)–C(22)	1.919 (13)	C(22)–O(22)	1.131 (17)
Os(2)–C(23)	1.881 (16)	C(23)–O(23)	1.150 (20)
Os(3)–C(31)	1.921 (6)	C(31)–O(31)	1.186 (19)
Os(3)–C(32)	1.919 (19)	C(32)–O(32)	1.128 (24)
Os(3)–C(33)	1.924 (15)	C(33)–O(33)	1.105 (19)
W–C(41)	1.972 (15)	C(41)–O(41)	1.192 (19)
(C) Metal–Carbon (μ_3-η^2-Alkyne) Distances			
Os(1)–C(3)	2.162 (10)	W–C(2)	2.149 (15)
Os(3)–C(2)	2.151 (12)	W–C(3)	2.188 (12)
		W···midpt[a]	2.053
(D) Tungsten–Carbon (Cp) Distances			
W–Cp(1)	2.293 (20)	Cp(1)–Cp(2)	1.431 (29)
W–Cp(2)	2.315 (18)	Cp(2)–Cp(3)	1.369 (30)
W–Cp(3)	2.371 (20)	Cp(3)–Cp(4)	1.392 (28)
W–Cp(4)	2.432 (19)	Cp(4)–Cp(5)	1.399 (25)
W–Cp(5)	2.348 (19)	Cp(5)–Cp(1)	1.349 (31)
W···centroid	2.034		
(E) Distances within $C_2(CO_2Et)_2$ Ligand			
C(2)–C(3)	1.399 (18)		
C(1)–C(2)	1.549 (19)	C(3)–C(4)	1.489 (16)
C(1)–O(1)	1.160 (18)	C(4)–O(3)	1.206 (17)
C(1)–O(2)	1.330 (18)	C(4)–O(4)	1.312 (16)
O(2)–C(5)	1.445 (24)	O(4)–C(7)	1.436 (18)
C(5)–C(6)	1.384 (39)	C(7)–C(8)	1.424 (28)
(F) M–H Distances			
Os(1)–H(12)	1.60 (13)	Os(2)–H(12)	2.00 (15)
Os(3)–H(12)	1.71 (13)		

[a] midpt = midpoint.

Table VIII. Selected Interatomic Angles (deg) for $CpWOs_3(CO)_{10}(\mu_3\text{-}\eta^2\text{-}C_2(CO_2Et)_2)H$

(A) Intermetallic Angles			
W–Os(1)–Os(2)	54.3	W–Os(3)–Os(1)	61.5
W–Os(1)–Os(3)	59.1	W–Os(3)–Os(2)	55.0
Os(2)–Os(1)–Os(3)	59.9	Os(1)–Os(3)–Os(2)	60.1
W–Os(2)–Os(1)	63.8	Os(1)–W–Os(2)	61.9
W–Os(2)–Os(3)	62.2	Os(1)–W–Os(3)	59.5
Os(1)–Os(2)–Os(3)	59.9	Os(2)–W–Os(3)	62.8
(B) M–C–O Angles			
Os(1)–C(11)–O(11)	177.1 (14)	Os(2)–C(23)–O(23)	176.8 (13)
Os(1)–C(12)–O(12)	174.2 (13)	Os(3)–C(31)–O(31)	175.4 (16)
Os(1)–C(13)–O(13)	170.7 (12)	Os(3)–C(32)–O(32)	179.4 (14)
Os(2)–C(21)–O(21)	176.5 (15)	Os(3)–C(33)–O(33)	179.0 (16)
Os(2)–C(22)–O(22)	173.0 (13)	W–C(41)–O(41)	178.4 (13)
(C) M–C(Alkyne)–M Angles			
W–C(2)–Os(3)	84.0 (5)	W–C(3)–Os(1)	85.3 (4)
(D) M–C–C Angles Associated with the Alkyne Ligand			
Os(3)–C(2)–C(3)	113.0 (8)	Os(1)–C(3)–C(2)	107.4 (7)
W–C(2)–C(3)	72.7 (8)	W–C(3)–C(2)	69.6 (8)
Os(3)–C(2)–C(1)	120.0 (9)	Os(1)–C(3)–C(4)	123.2 (8)
(E) C–C–C Angles within the μ_3-η^2-Alkyne System			
C(1)–C(2)–C(3)	125.6 (11)	C(4)–C(3)–C(2)	124.3 (11)
C(2)–C(1)–O(1)	124.3 (13)	C(3)–C(4)–O(3)	122.1 (12)
C(2)–C(1)–O(2)	110.6 (12)	C(3)–C(4)–O(4)	116.0 (11)
O(1)–C(1)–O(2)	125.0 (14)	O(3)–C(4)–O(4)	121.8 (12)
C(1)–O(2)–C(5)	117.6 (13)	C(4)–O(4)–C(7)	117.9 (11)
O(2)–C(5)–C(6)	110.5 (22)	O(4)–C(7)–C(8)	108.3 (15)
(F) Cp(centroid)–W–Os Angles			
cent–W–Os(1)	176.1	cent–W–Os(3)	123.7
cent–W–Os(2)	116.8		

---

(16) Park, J. T.; Shapley, J. R.; Churchill, M. R.; Bueno, C. *Inorg. Chem.* 1984, *23*, 4476.

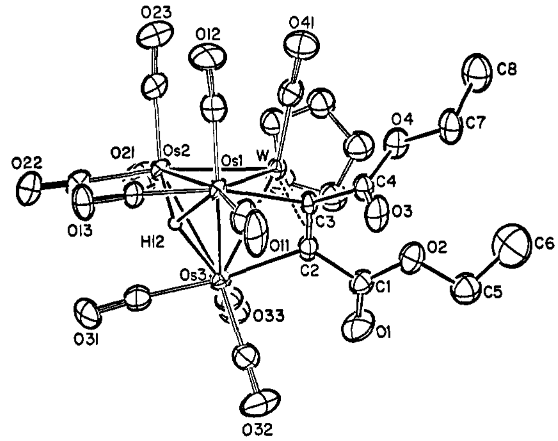

Figure 4. Labeling of atoms and molecular geometry of CpWOs$_3$(CO)$_{10}$(μ_3-η^2-C$_2$(CO$_2$Et)$_2$)H (**6b**).

The WOs$_3$ system defines a tetrahedral cluster and is associated with 60 outer valence electrons. The X-ray diffraction study suggests that the hydride ligand is associated with the Os$_3$ face. Each osmium atom bears three terminal carbonyl ligands while W has only one. The μ_3-η^2-C$_2$(CO$_2$Et)$_2$ ligands lies on a WOs$_2$ face and is formally π-bonded to W (W–C(2) = 2.149 (15), W–C(3) = 2.188 (12), and W···midpoint = 2.053 Å) and σ-bonded to Os(1) and Os(3) (Os(1)–C(3) = 2.162 (10) and Os(3)–C(2) = 2.151 (12) Å).

Formal electron counts at the metal atoms reveal particularly that Os(2) is electron-deficient and that W is electron-precise. In this molecule, the problem appears to be compensated for solely by donation of electron density directly from tungsten to Os(2), as is indicated by the very short W–Os(2) bond (W–Os(2) = 2.665 (1) Å as compared to W–Os(1) = 2.947 (1) and W–Os(3) = 2.878 (1) Å). Note that, apart from the W–Os(2) bond, the variation in M–M bond lengths is very small, with the other five bonds being in the range 2.878 (1)–2.947 (1) Å. The situation is clearly different from that in CpWOs$_3$(CO)$_{10}$(μ_3-η^2-C$_2$Tol$_2$)H (**1a**), where M–M distances are 2.647 (3)–2.663 (3) Å for the equivalent "short" W–Os bond and range from 2.775 (3) through 3.095 (3) Å for the remaining five linkages; it is, perhaps, this property which leads to the "unsymmetric" isomer being thermodynamically more stable than the "symmetric" isomer.

The EtO$_2$CC≡CCO$_2$Et ligand is bent with ∠C(1)–C(21)–C(3) = 125.6 (11)° and ∠C(2)–C(3)–C(4) = 124.3 (11)°; the original alkyne linkage is now lengthened to C(2)–C(3) = 1.399 (18) Å. Other distances and angles are in the expected ranges and are substantially more accurate and precise than those for **1a** because of superior crystal quality and concomitantly higher resolution. Thus, Os–CO = 1.881 (16)–1.924 (17) Å (average = 1.908 ± 0.017 Å) and C–O = 1.108 (20)–1.192 (19) Å (average = 1.143 ± 0.033 Å). All M–C–O systems are close to linear, with angles ranging from 170.7 (12) through 179.4 (14)°.

Isomerization. Symmetrical isomers **5a**, **6a**, and **7a** change irreversibly to unsymmetrical isomers **5b**/**5c**, **6b**, and **7b** upon heating. For the isomerization of **6a** to **6b** kinetic measurements were carried out on samples sealed in NMR tubes and heated at 100 °C. No difference in the rate of isomerization was observed between a sample sealed under vacuum and one sealed under an atmosphere of carbon monoxide. The isomerization reaction of **6a** was examined also in the presence of excess di-*p*-tolylacetylene in refluxing toluene. There was no evidence for the formation of **1a**, which might have been expected if alkyne exchange had occurred.

Detailed speculation about the mechanism of isomerization cannot be supported. However, one possibility is "insertion" of the alkyne into either the Os(1)–Os(3) or the Os(1)–Os(2) bond to give an intermediate with μ_4-η^2-bonding mode I. This structure involves the same number of skeletal electron pairs (seven) as the observed μ_3-η^2-bonding mode II. On the other hand, insertion of the alkyne into the metal hydride bond would give an intermediate vinylic complex that could facilitate movement of the C$_2$R$_2$ moiety over the cluster framework.

The isomerization occurs only for the clusters derived from alkynes with highly electron-withdrawing substituents (R = CO$_2$Et or CF$_3$). In isomer **a**, the position of carbonyl region IR absorption bands reflects an electronic effect due to the coordinated alkyne. The corresponding most intense bands for **1a**–**7a** were observed in the following order

$$\underset{2019\ \text{cm}^{-1}}{\text{TolC}{\equiv}\text{CTol}} < \underset{2020\ \text{cm}^{-1}}{\text{PhC}{\equiv}\text{CPh}} \approx \underset{2020\ \text{cm}^{-1}}{\text{TolC}{\equiv}\text{CPh}} < \underset{2021\ \text{cm}^{-1}}{\text{HC}{\equiv}\text{CH}} <$$
$$\underset{2031\ \text{cm}^{-1}}{\text{PhC}{\equiv}\text{CCO}_2\text{Et}} < \underset{2037\ \text{cm}^{-1}}{\text{EtO}_2\text{CC}{\equiv}\text{CCO}_2\text{Et}} < \underset{2043\ \text{cm}^{-1}}{\text{F}_3\text{CC}{\equiv}\text{CCF}_3}$$

In the structure of symmetrical isomer **1a**, the alkyne is π-bonded to a formally electron-deficient osmium center. However, in the structure of the unsymmetrical isomer **6b**, the alkyne is π-bonded to the electron-precise (18-electron) tungsten center. The relative strengths of the π-interactions for electron-withdrawing alkynes could be reflected in the relative stabilities of isomers **a** and **b**.

Scission of Alkyne Ligands. The diaryl alkyne WOs$_3$ clusters **1a**–**3a** undergo scission of the alkyne ligand to provide dialkylidyne compounds CpWOs$_3$(CO)$_9$(μ_3-CR)(μ_3-CR′)H (**1d**, R = R′ = Tol; **2d**, R = R′ = Ph; **3d**, R = Ph, R′ = Tol). Compound **1d** has been obtained previously by an entirely different route and was shown to have a terminal hydride on the tungsten atom.[16] The dialkylidyne clusters are obtained in low yields (10–20%) by direct pyrolysis of the corresponding alkyne complexes either in solution (toluene, 110 °C) or in vacuo (hot tube, 250 °C). However, initial decarbonylation with Me$_3$NO/MeCN followed by pyrolysis in refluxing toluene results in formation of the dialkylidyne clusters as the major products (ca. 60%) along with the corresponding alkyne–oxo clusters CpWOs$_3$(CO)$_8$(μ-O)(μ_3-η^2-C$_2$RR′)H (**1e**, R = R′ = Tol; **2e**, R = R′ = Ph) (ca. 10%) according to eq 6. An attempted alkyne scission reaction of **4a** resulted only in the ethyne–oxo cluster (**4e**, R = R′ = H) as an isolated product, and the compound has been structurally and spectroscopically characterized.[4b] The alkyne–oxo clusters **1e** and **2e** were isolated as dark red solids, and their formulations were estabilished by spectroscopic data. Close similarities between the IR spectra of **1e** and **2e** with

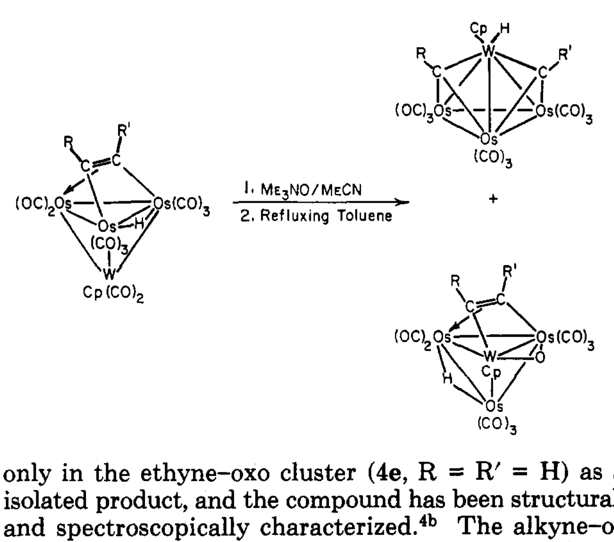

(6)

that of **4e** indicate strongly that **1e** and **2e** adopt structures analogous to that of **4e**.

The observation that phyrolysis of the phenyltolylacetylene complex **3a** gives only **3d** and none of the **1d** or **2d** implies that the alkyne scission process occurs without extensive fragmentation of the metal framework. Further details, however, are sketchy at best. Preliminary work suggests that initial decarbonylation with Me$_3$NO/MeCN occurs at Os(1) or Os(2),[17] but the overall result requires complete decarbonylation at tungsten. Thus, further carbonyl exchange, either intramolecular or intermolecular, is involved.

The presence of the tungsten atom in the cluster certainly appears to facilitate alkyne scission.[3d] It has been suggested by Fehlner and co-workers that the carbon–carbon bond scission of alkyne moieties in metal clusters, in carboranes, and on metal surfaces is driven by charge transfer (M → π*) from the relatively electropositive metal or boron atoms to the resulting alkylidyne ligands.[18] The tungsten atom in the dialkylidyne complex CpWOs$_3$(CO)$_9$(CR)(CR′) can be viewed as being bound to six anionic ligands (C$_5$H$_5^-$, H$^-$, 2C$^-$, 2Os$^-$) and a neutral donor Os center. The formal oxidation state of the tungsten center is +6. Thus, the results involving alkyne scission on the tungsten–triosmium clusters appear to be consistent with this idea in that the alkylidyne ligands are coordinated to a relatively oxidized, more electropositive, tungsten. The results of Fehlner and co-workers also suggest that the degree of M → π* charge transfer increases as the number of metal atoms to which the alkyne is coordinated increases and that the sites permitting the greatest number of metal–alkylidyne carbon interactions will be most effective in carrying out scission of the coordinated alkyne. Therefore a pseudoctahedral species with configuration I (probably unsaturated) may be an important intermediate in the alkyne scission reaction.

Registry No. **1a**, 86885-45-2; **1a***, 116025-81-1; **1d**, 86885-48-5; **1e**, 116052-47-2; **2a**, 86885-46-3; **2a***, 116025-82-2; **2d**, 86885-49-6; **2d***, 116025-83-3; **2e**, 116052-48-3; **3a**, 86885-47-4; **3d**, 86885-50-9; **5a**, 116025-75-3; **5b**, 116025-76-4; **5c**, 116126-24-0; **6a**, 116025-77-5; **6b**, 116025-78-6; **7a**, 116025-79-7; **7b**, 116025-80-0; CpWO$_{53}$(CO)$_{12}$H, 68796-10-1; CPWO$_{53}$(CO)$_{12}$H (^{13}C enriched), 116102-23-9; Os, 7440-04-2; W, 7440-33-7; di-*p*-tolylacetylene, 2789-88-0; diphenylacetylene, 501-65-5; phenyl-*p*-tolylacetylene, 3287-02-3; ethyl phenylpropiolate, 2216-94-6; diethyl acetylenedicarboxylate, 762-21-0; hexafluoro-2-butyne, 692-50-2.

Supplementary Material Available: Tables of anisotropic thermal parameters for **1a** and **6b** and additional distances and angles for **1a** (5 pages); listings of structure factors **1a** and **6b** (56 pages). Ordering information is given on any current masthead page.

---

(17) Koerner, P. J. M.S. Thesis, University of Illinois, 1987.

(18) Deshmukh, P.; Dutta, T. K.; Hwang, J. L.-S.; Housecroft, C. E.; Fehlner, T. P. *J. Am. Chem. Soc.* **1982**, *104*, 1740.

Electronic Structures and Reactivities of (η^5-2,3,5-Tricarbahexaboranyl)nickel Sandwich Complexes. A Combined Electrochemical, Preparative, and NMR Spectroscopic Approach[1]

Joachim Zwecker, Thomas Kuhlmann, Hans Pritzkow, Walter Siebert,* and Ulrich Zenneck*

Anorganisch Chemisches Institut der Universität, D-6900 Heidelberg, Federal Republic of Germany

Received February 29, 1988

(μ-η^5-1,3-Dimethyl-4,5-diethyl-2,3-dihydro-1,3-diborolyl)bis[(η^5-1,4,6-trimethyl-2,3-diethyl-2,3,5-tricarbahexaboranyl)nickel] (**1**) may be cleaved in the presence of 1,5-cyclooctadiene by chemical or electrochemical oxidation to form (η^5-1,4,6-trimethyl-2,3-diethyl-2,3,5-tricarbahexaboranyl)(η^5-1,3-dimethyl-4,5-diethyl-2,3-dihydro-1,3-diborolyl)nickel (**4**) and (η^5-1,4,6-trimethyl-2,3-diethyl-2,3,5-tricarbahexaboranyl)(1,5-cyclooctadiene)nickel(1+) (**5**$^+$) in good yields. This reaction has been monitored by cyclic voltammetry, coulometry, and controlled potential electrolysis. **4** and **5**$^+$BF$_4^-$ have been characterized fully, including single-crystal X-ray diffraction studies. **4**: space group $P\bar{1}$, $Z = 2$, $a = 9.055$ (3) Å, $b = 11.140$ (4) Å, $c = 13.406$ (4) Å, $\alpha = 103.36$ (3)°, $\beta = 105.61$ (2)°, $\gamma = 109.91$ (3)°, $V = 1144.1$ Å^3, $R = 0.034$, $R_w = 0.030$. **5**$^+$BF$_4^-$: space group $C2/c$, $Z = 8$, $a = 15.418$ (2) Å, $b = 14.331$ (3) Å, $c = 19.809$ (5) Å, $\alpha = 90°$, $\beta = 103.78$ (2)°, $\gamma = 90°$, $V = 4250.9$ Å^3, $R = 0.056$, $R_w = 0.048$. The reaction of **4** and bis(carbonylcyclopentadienylnickel) yields the asymmetric triple-decker complex (μ-η^5-1,3-dimethyl-4,5-diethyl-2,3-dihydrodiborolyl)(η^5-1,4,6-trimethyl-2,3-diethyl-2,3,5-tricarbahexaboranyl)nickel(η^5-cyclopentadienyl)nickel (**8**). The combination of electrochemistry and paramagnetic NMR spectroscopy on **1**, **8**, and (μ-η^5-1,3-dimethyl-4,5-diethyl-2,3-dihydro-1,3-diborolyl)bis(cyclopentadienylnickel) (**2**) as well as electrochemistry of **4** and **5**$^+$ and ESR spectroscopy of their redox products allows a precise description of the properties of the 1,4,6-trimethyl-2,3-diethyl-2,3,5-tricarbahexaboranyl ligand. It is isolobal in respect to the cyclopentadienyl ligand, and the energies of the MO's involved in metal–ligand bonding are nearly identical for both ligands.

Introduction

Electrochemistry now is a well-established tool to investigate electron-transfer reactions even of precious organometallics like polynuclear organotransition-metal complexes[3] or metallaborane cage compounds.[4] In prin-

---

(1) Redox Chemistry of Transition-Metal π-Complexes. 1. (Tricarbahexaboranyl)metal Complexes. 2. Part 1: see ref 2.

(2) Zwecker, J.; Pritzkow, H.; Zenneck, U.; Siebert, W. *Angew. Chem.* **1986**, *98*, 1129; *Angew. Chem., Int. Ed. Engl.* **1986**, *25*, 1099.

(3) Geiger, W. E.; Connelly, N. G. *Adv. Organomet. Chem.* **1984**, *123*, 1; **1985**, *124*, 86.

0276-7333/88/2307-2316$01.50/0